The repulsive wall of the Ar–Ar interatomic potential reexamined

Ronald A. Aziz and M. J. Slaman

The repulsive wall of the Ar–Ar interatomic potential reexamined

Ronald A. Aziz[a] and M. J. Slaman
Department of Physics, University of Waterloo, Waterloo, Ontario, N2L 3G1

The repulsive wall of the Ar–Ar interaction is reexamined with the purpose of rationalizing the apparent inconsistency between high energy beam results and high temperature transport data. A new piece-wise experimental potential is proposed which predicts not only the beam results but a large set of transport data up to 7000 K. Lower temperature/energy data are predicted almost equally as well as other state-of-the-art empirical potentials.

I. INTRODUCTION

Current interest in rare gas solids at high pressures has focused attention on the repulsive wall of the pair potential. For only if that is accurately known will one be able to determine which assumptions concerning the many-body forces are valid for the solid. In particular, there has been considerable controversy over the past decade and a half about the location of the repulsive wall of the Ar–Ar interaction. The evolution of the thinking on the repulsive wall will be reviewed.

Barker, Fisher, and Watts[1] (BFW) fitted the repulsive wall of their potential (BFW) to the earlier beam work of Amdur and coworkers.[2,3] These data give rise to a wall appreciably lower (25% at 1.7 A to 1.5% at 2.65 A) than the beam potential determined by Rol and co-workers[4] several years later. About the same time, Aziz[5] demonstrated that, if the wall of the BFW potential was made harder by splining onto it an exponential function of Born–Mayer form, then the predictability of many of the transport properties were improved. In particular, the high temperature thermal diffusion data of Taylor and Weissman[6] which sense the repulsive wall up to about 4500 K are more consistent with a harder wall.

Aziz and Chen[7] then fitted simple functional forms of the Hartree–Fock-dispersion variety (HFD-C and HFD-B) to precise spectroscopic data (vibration–rotation spectrum) for the argon dimer measured by Colbourn and Douglas[8] and the high temperature viscosity correlation of Maitland and Smith.[9] The long-range interaction was constrained within the bounds of Tang et al.[10] and the "Hartree–Fock component" constrained close to the *ab initio* self-consistent-field (SCF) calculations at short range due to Wahl.[11] The potential was able to predict many other sets of data available at that time with high precision. It also predicts a number of sets of data subsequently measured including the glory structure in the total cross sections (TCS)[12] and the shock-tube thermal conductivity data (to 5350 K) of Cavero et al.,[13] Hirschberg (to 6600 K)[14] and of the Prague group (to 7000 K).[15] In the same paper, Aziz and Chen softened the repulsive wall (HFD-D potential) in order to reproduce the high energy beam potential of Rol and coworkers.[4] The softened potential did not predict the high

temperature viscosity correlations of Maitland and Smith[9] and Hanley[16] nor the shock-tube thermal conductivity as well as the harder HFD-C potential. As a result, it was deemed at that time to be an unacceptable potential.

However, Ross et al.[17] found that when the repulsive wall of either the BFW or HFD-C were modified by smoothly joining on the Rol beam potential, their Hugoniot curves could be accounted for by treating this composite potential as an "effective" pair-wise additive potential. In other words, no many-body terms were included in their calculations. If this composite potential were indeed the true pair potential, then Ross suggested that "many-body exchange or multipole interactions in dense argon, if present, are negligible to within experimental accuracy". But this suggestion seemed to be contrary to conventional wisdom. Moreover, Ross[18] noted, from his work on He and H_2, that many-body repulsive forces tend to make a significant negative contribution at high density. It might then be possible for the harder HFD-C to be consistent with the thermal conductivity data and the dense shock data.

Model potentials which were subsequently proposed all have repulsive walls which are more or less as hard as the HFD-C potential. These include the model potentials of Koide et al.,[19] Douketis et al.,[20] and Tang and Toennies.[21] As a result of the availability of new data, Aziz and Slaman[22] presented a refined potential (HFD-B2). It incorporated new dispersion coefficients (C_6 of Kumar and Meath[23] and C_8 and C_{10} values within the bounds provided by Standard and Certain[24]). It was then fitted to the precise viscosity values of Vogel.[25] The resulting potential provided a better fit to the spectroscopic data of Colbourn and Douglas.[8] The new HFD-B2 potential is slightly less repulsive than the original HFD-C. In addition, the "SCF component" of either potential agrees rather closely with *ab initio* SCF calculations of Wahl,[11] Wadt,[26] Ahlrichs et al.,[27] and Hay et al.[28]

Much of the above seemed to weigh heavily in favor of the more repulsive potentials and against the beam potential of Rol and coworkers. Then there were a number of developments which suggest that the reverse might indeed to be the case. In the case of helium and helium-noble gases, the work of Stebbings and co-workers[29] on very high energy (~0.5 keV) differential cross sections favors Rol's beam potentials. In addition, Ceperley and Partridge[30] used Monte Carlo techniques to determine Born–Oppenheimer interaction energies for helium at separations of 1.0 to 3.0 bohr. These

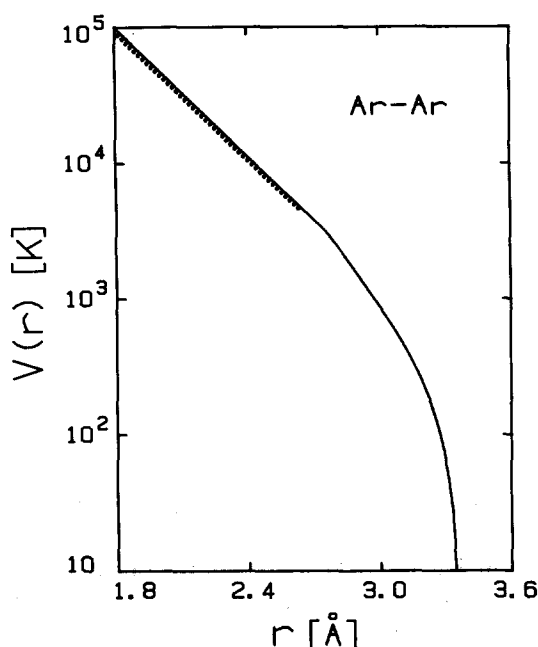---

[a] Author to whom correspondence should be addressed.

FIG. 1. The repulsive wall of the Ar–Ar potential. The beam potential of Rol and co-workers (large dots) (Ref. 4). The present HFDTCS2 potential (solid line).

values are less than the beam values but are within 5% of them at about 1–1.75 bohr. In the case of argon, McLean et al.[31] calculated high quality ab initio values of the argon potential at separations of 3–30 bohr. In the region considered most accurate (3–6 bohr), the values were somewhat higher than Rol's values but substantially less than the potentials of Refs. 19–22. At 5 bohr, their calculated value agrees with Rol's value to within 3%.

Aziz et al.[32] and Aziz and Slaman[33] constructed high quality empirical potentials for helium and xenon, respectively. For helium, the wall was pinned to Ceperley and Partridge's value at a separation of 1 bohr. The resultant potential is softer than the beam potential of Rol by about 6% or less in the range of 1–2 bohr, then drops off to about 18% lower near 3 bohr but, in general, slightly harder than Ceperley and Partridge's results. The repulsive wall of xenon was kept to within about 10% of the beam potential. Barker[34] modified this potential for xenon so that its repulsive wall is closer to Rol's results in the region for which separations are 2.4–3.0 Å. He found that, with this modification, he achieved better agreement with high pressure equation of state measurements when only the Axilrod Teller interaction was included. Further work is currently in progress to get closer agreement with the beam results.[35]

In view of the foregoing preamble, it seems desirable to construct potentials for argon with a repulsive wall more consistent with the beam data of Ref. 4 while still maintaining the accuracy of the well and the low repulsive wall. Initially, we fitted as much as we could of the reliable experimental data with a single-function potential of the HFD-B form (HFD-B3). This approach has merit from a computational point of view. However, this somewhat inflexible potential did not characterize high temperature transport data as well as we would like. To allow for more flexibility in the repulsive wall, we employed a piece-wise form (HFDTCS)

which consists of our new HFD-B potential connected to the TCS beam potential (expressed in Born–Mayer form) by means of an exponential cubic spline. The beam potential has error bars of ± 10% and when it is used at its upper limit, we were able to construct a potential which can reproduce all important sets of microscopic and macroscopic data.

II. THE POTENTIALS

The single-function potential form used to describe the Ar–Ar interaction is the HFD-B variety of Aziz and Chen.[1] The form of the potential is

$$V(r) = \epsilon V^*(x),\qquad(1)$$

where

$$V^*(x) = A^* \exp(-\alpha^* x + \beta^* x^2)$$
$$- F(x)\sum_{j=o}^{2} c_{2j+6}/x^{2j+6},\qquad(2)$$

with

$$F(x) = \exp\left[-(D/x - 1)^2\right],\quad x < D,$$
$$= 1,\quad x < D,\qquad(3)$$

with $x = r/r_m$ and $r_m = 3.761$ Å.

Differences in the repulsive wall will affect the prediction of viscosity and especially the high temperature values.[36,37] The data of Vogel[25] are considered to be superior to other data in the temperature range 298–623 K and all potentials should predict these. The fitting procedure has been described fully by Aziz and Slaman.[22] We will dub this potential the "HFD-B3". Parameters for the HFD-B3 potential are presented in Table I.

The HFD-B3 potential, as discussed in the next section, predicts all properties except high temperature transport data. Even though the HFD-B3 lies within the error bars of Rol's results, a potential (HFDTCS1) that reproduces these data exactly may be desirable for high pressure studies. To create such a potential, we make use of a piece-wise composite potential which connects the HFD-B3 to the beam results

TABLE I. Parameters for the HFD-B Ar–Ar potentials.

	HFD-B3	HFD-B4
A^*	1.13 211 845 (5)[a]	1.679 345 97 (5)
α^*	9.00 053 441	10.140 587 22
c_6	1.09 971 113	1.099 711 13
c_8	0.54 511 632	0.567 124 12
c_{10}	0.39 278 653	0.408 203 07
C_6 (a.u.)	64.3	64.3
C_8 (a.u.)	1610	1675
C_{10} (a.u.)	58 600	60 900
β^*	− 2.602 702 26	− 1.844 523 78
β [Å^{-2}]	− 0.1840	− 0.1304
D	1.0400	1.116
ϵ/K (K)	143.25	143.25
r_m (Å)	3.761	3.761
σ (Å)	3.356$_0$	3.352$_5$

[a] Not all figures displayed are significant. Some are included only to avoid round off errors. (5) means 10^5.

TABLE II. (a) Parameters for the exponential cubic spline valid in the region $r_1 < r < r_2$ of Eq. (6). (b) Parameters (unreduced) for the Born–Mayer Component.

(a) Piece-wise Potential	r_1 (Å)	r_2 (Å)	a_1	a_2	a_3	a_4
HFDTCS1	2.65	2.70	3.388 9786	− 14.199 649	− 50.214 717	− 3546.530 51
HFDTCS2	2.73	2.98	3.179 0298	− 18.991 157	− 80.983 465	1044.136 19
HFDICF	2.73	2.98	3.058 8126	− 17.182 906	− 6.693 638	− 482.749 43

(b)	B (eV)	b (Å^{-1})
HFDTCS1	5060	3.598
HFDTCS2	5780	3.6182

(TCS) of Rol *et al.* (in Born–Mayer form) via an exponential cubic spline function.

The form of the potential is

$$V(r) = \epsilon V^*(x) \tag{4}$$

and

$$V^*(x) = B * \exp[- b^* x], \qquad\qquad x < x_1, \tag{5}$$

$$V^*(x) = \exp\{a_1 + (x - x_1)(a_2 + (x - x_2)$$
$$\times [a_3 + (x - x_1)a_4])\}, \qquad x_1 \leqslant x \leqslant x_2, \tag{6}$$

$$V^*(x) = V^*_{\text{HFD-B3}}(x), \qquad\qquad x > x_2, \tag{7}$$

where

$$x = r/r_m$$

and

$$r_m = 3.761 \, A.$$

While this form has the flexibility to reproduce those results exactly, we found that this potential (HFDTCS1) was not repulsive enough to fit the high temperature transport data simultaneously. However, by approaching the upper limit of the TCS data, we were able to predict the transport data in addition. The spline functions are chosen in the wall of the potential in such a way that agreement with Vogel's[25] viscosity data is maintained and that agreement with the high temperature Los Alamos viscosity[38] is achieved. This potential is dubbed the HFDTCS2. The parameters for the HFD component of the HFDTCS1 and HFDTCS2 potentials are identical to those of the HFD-B3 potential. (See Table I). The parameters for the spline components are given in Table II.

An alternate potential (HFD-B4) of the same form as the HFD-B3 is presented in the event that the calculations of McLean *et al.*[31] prove to define better the location of the repulsive wall. The HFD-B4 potential is constructed so that its repulsive wall is located as closely as possible to the *ab initio* potential of McLean *et al.* but is, in all other respects, almost identical to the "experimental" HFD-B3 potential. The parameters for this potential are given in Table I.

For the sake of completeness, a piece-wise potential (HFDICF) which connects the HFD-B3 potential to the smoothed interacting correlated fragments (ICF) calculations of McLean *et al.* with a spline is also presented. The parameters for the spline component of the HFDICF potential are given in Table II.

For separations less than 1.7 A, there appears to be no experimental data to which a potential can be fitted. Because of this and the tendency of many potential forms to behave unrealistically at these small separations, it is desirable to obtain a more physically based representation of the potential energy curve in this region. This can be done by making use of the united atom perturbation theory results (UAPT) of Pathak and Thakkar.[39] Following Pathak and Thakkar, we can connect their UAPT results for argon (valid between $r = 0.003$–0.21 Å or 0.005–0.4 bohr) to the present HFD-B3, HFD-B4, HFDTCS, and HFDICF potentials with an interpolation function. The functional forms and their parameters are given in the Appendix.

TABLE III. Value of highly repulsive region of $V(r)$ in K. Percentage deviations of various potentials from "beam" values of Rol and co-workers.[4]

r(Å)	Rol *et al.*	%err	HFD-B3	HFDTCS2	HFD-B2	HFD-C	HFD-D	BFW	ICF-AS	HFD-B4
1.70	129 530	10	− 5.62[a]	10.37[a]	28.60	30.52	− 4.38[a]	− 25.58	0.35[a]	9.72[a]
1.80	90 390	10	− 3.43[a]	10.15[a]	30.60	34.39	− 0.63[a]	− 28.52	7.06[a]	10.70
1.90	63 070	10	− 1.01[a]	9.93[a]	31.85	37.11	2.73[a]	− 27.91	12.35	11.57
2.00	44 010	10	1.43[a]	9.71[a]	32.34	38.65	5.62[a]	− 24.79	16.07	12.29
2.10	30 710	10	3.67[a]	9.48[a]	32.02	39.01	7.93[a]	− 20.14	18.18	12.74
2.20	21 430	10	5.47[a]	9.26[a]	30.85	38.19	9.50[a]	− 14.81	18.66	12.78
2.30	14 960	10	6.59[a]	9.04[a]	28.75	36.14	10.17[a]	− 9.59[a]	17.55	12.21
2.40	10 440	10	5.77[a]	8.82[a]	25.62	32.83	9.76[a]	− 5.17[a]	14.90	10.85
2.50	7 283	10	3.31[a]	8.60[a]	21.34	28.17	8.06[a]	− 2.16[a]	10.78	8.47[a]
2.65	4 245	10	1.45[a]	8.28[a]	12.38	18.39	2.66[a]	− 1.44[a]	1.91[a]	2.44[a]

[a] Denotes agreement with experiment.

TABLE IV. Value of highly repulsive region of $V(r)$ in K. Percentage deviations of various potentials from ICF values of McLean et al.[31]

r(a.u.)	ICF	%err	ICF-AS	HFD-B4	HFD-C	HFD-D	HFD-B3	HFD-B2	BFW	HFDTCS2
3.5	83 065	0.22	− 0.77	0.28	22.46	− 8.73	− 11.76	18.49	− 35.57	− 0.74
4.0	33 786	0.23	1.33	− 3.46	18.77	− 7.34	− 10.97	12.90	− 30.90	− 6.31
4.5	12 797	0.45	0.76	− 3.02	16.33	− 4.11	− 6.82	10.17	− 17.92	− 5.03
4.75	7 636	0.72	0.01[a]	− 1.86	15.57	− 2.16	− 4.16	9.59	− 10.89	− 1.39
5.00	4 436	1.16	− 0.73[a]	− 0.29	15.13	− 0.09[a]	− 1.29	9.44	− 4.22	5.18
5.25	2 486	2.05	− 1.20[a]	1.57[a]	15.02	2.04[a]	1.68[a]	9.66	1.83[a]	13.72
5.50	1 320	3.61	− 1.16[a]	3.64[a]	15.29	4.20	4.73	10.18	7.15	7.74
5.75	638.9	6.82	− 0.36[a]	5.86[a]	16.08	6.35	7.90	10.99	11.98	7.90
6.00	253.2	15.4	1.43[a]	8.30[a]	18.10	8.57	11.70[a]	12.23[a]	17.43	11.70[a]
6.25	43.9	78.1	3.84	12.87[a]	30.71[a]	12.10[a]	23.25[a]	16.26[a]	37.77[a]	23.35[a]

[a] Denotes agreement with ICF values.

III. RESULTS AND DISCUSSION
A. The highly repulsive wall

The repulsive walls of the HFD-B2, HFD-B3, HFD-B4, HFD-C, HFD-D, BFW, ICF-AS, and HFDTCS2 potentials are compared with that of Rol and coworkers[4] in Table III. (McLean et al.[31] proposed a hybrid potential (ICF-AS) which reproduces approximately their ICF potential ob-tained using the method of interacting correlated fragments and joins onto the HFD-B2 potential (AS) of Aziz and Slaman at a separation of 3:43 Å) It is seen that, of the single-function potentials, the HFD-B3 is the closest to the beam potential and is no further than 6.8% from it. The new HFD-B3 is less repulsive than either the HFD-C or HFD-B2 potential in the relevant region (see Table III). In addition, the HFD-D, HFDTCS, and HFDTCS2 are the only others

TABLE V. A summary of the predictive ability of various Ar–Ar potentials. The entry "Yes" means agreement with experiment, etc.

Data	Temperature range (K)	Estimated or expected error bars (%)	Maximum ± % Deviation for HFDTCS2 potential Present and Recommended	HFDTCS2 Present and Recommended	HFD-B2	HFD-B3 Present	HFD-B4 Present	HFD-C	HFD-D	HFDTCS1 Present	ICF-AS	HFDICF Present	BFW
Bean data													
Rol and co-workers (Ref. 4)	n/a	± 10	8.3 to 10.4	Yes	No	Yes	No	No	Yes	Yes	No	No	No
Viscosity (raw data)													
Vogel (Ref. 25)	298–628	± 1.0 to ± 0.3	− 0.04 to 0.31	Yes	Yes	Yes	Yes	No	Yes	Yes	No	Yes	No
Guevara et al. (Ref. 38)[a]	1100–2100	± 1 (Est)	− 0.97 to 0.38	Yes	Yes	No	No	No	No	No	No	No	Almost
Dawe and Smith (Ref. 40)[a]	300–1600	± 1	− 0.31 to 1.36	No	No	No	No	Yes	No	No	No	No	No
Viscosity (correlation data)													
Najafi et al. (Ref. 42)	200–4400	± 1	− 0.52 to 0.82	Yes	Yes	No	No	Yes	No	No	No	No	No
Hanley (Ref. 16)	100–1000	± 1	− 0.74 to − 0.02	Yes	Yes	Yes	Yes	No	Yes	Yes	Yes	Yes	No
Hanley (Ref. 16)	1000–2000	± 1¼	− 0.02 to 0.74	Yes	Almost	No	No	Yes	No	No	No	No	Yes
Maitland and Smith (Ref. 9)	200–600	± 1	− 0.54 to 0.14	Yes	Yes	Yes	Yes	Yes	Yes	Yes	Yes	Yes	Yes
Maitland and Smith (Ref. 9)	600–2200	± 1¼	0.14 to 1.00	Yes	Yes	No	No	Yes	No	No	No	No	No
Watson (Ref. 43)	250–1800	± 1 (Est)	− 0.64 to 0.97	Yes	No	No	No	Yes	No	No	No	No	No
Thermal Conductivity (Raw Data)													
Chen and Saxena (Ref. 44)	400–2500	± 1.5	− 1.17 to 1.33	Yes	No	No	No	No	No	No	No	No	No
Vargaftik and Zimina (Ref. 45)	273–1273	± 1 (Est)	− 0.34 to 0.49	Yes	Yes	Yes	Yes	Yes	Yes	Yes	No	Yes	Yes
Springer and Wingeier (Ref. 46)	1100–2500	± 1 (Est)	− 0.93 to 0.43	Yes	No	No	No	No	No	No	No	No	No
Mastovsky (Ref. 15)	1500–7000	± 3 (Est)	− 0.74 to 2.29	Yes	Yes	No	No	Yes	No	No	No	No	No
Cavero et al. (SPM) (Ref. 13)	2900–5350	± 3 (Est)	2.52 to 2.82	Yes	Yes	No	No	Yes	No	No	No	No	No
Cavero et al. (MRM) (Ref. 13)	3700–5350	± 3 (Est)	1.71 to 1.80	Yes	Yes	No	Yes	Yes	Yes	No	No	No	No
Hirschberg (Ref. 14)	1550–2100	± 3	− 0.37 to 6.21	No	No	No	No	No	No	No	No	No	No
Hirschberg (Ref. 14)	5000–6400	± 3	1.95 to 5.26	No	No	No	No	Yes	No	No	No	No	No
Collins and Menard (Ref. 47)	1500–5000	± 5	1.03 to 3.93	Yes	Yes	Yes	Yes	Yes	Yes	Yes	Almost	Yes	Yes
Hoshino et al. (Ref. 48)	1100–4500	± 7	− 9.62 to − 0.62	No	No	No	Yes	No	No	No	No	No	No
Thermal Conductivity (Correlation Data)													
Kestin et al. (Ref. 49)	200–3273	± 1 (Est)	− 0.47 to 0.56	Yes	Yes	No	No	Yes	No	No	No	No	No
Watson (Ref. 43)	250–2000	± 1 (Est)	− 0.70 to 0.82	Yes	No	No	No	Almost	No	No	No	No	No
Varagaftik (Ref. 50)	200–5000	± 2 (Est)	− 1.63 to 2.02	Yes	Yes	No	No	No	No	No	No	No	No
Hanley (Ref. 16)	100–1000	± 1	− 0.72 to − 0.04	Yes	Yes	Yes	Yes	No	Yes	Yes	Yes	Yes	No
Hanley (Ref. 16)	1000–2000	± 1¼	− 0.04 to 0.68	Yes	Yes	No	No	Yes	No	Yes	No	No	Yes

[a] Relative measurements. Restated in terms of Vogel's results at room temperature.

TABLE VI. Parameters (in a.u.) for the interpolation function (A2) for the region $r_1 \leqslant r \leqslant r_2$. $V(r)$ is in Hartree.

Potential	r_1 (a.u.)	r_2 (a.u.)	b_1	b_2	b_3	β
HFD-B3	0.40	3.20	$-1.787\,99$	$1.036\,63$	$-0.149\,75$	$1.728\,32$
HFD-B4	0.40	3.50	$-1.778\,57$	$1.019\,56$	$-0.140\,35$	$1.737\,59$
HFDTCS1	0.40	3.20	$-1.823\,91$	$1.089\,21$	$-0.164\,62$	$1.688\,87$
HFDTCS2	0.40	3.20	$-1.844\,46$	$1.118\,14$	$-0.170\,95$	$1.665\,74$
HFDICF	0.40	3.50	$-1.711\,35$	$0.920\,44$	$-0.109\,52$	$1.809\,95$

which lie within the 10% error bars.

The repulsive walls of the ICF-AS, the HFD-B4, the BFW, and the various experimental HFD potentials are compared in Table IV from 3.5–6.25 bohr with the unsmoothed ICF calculations of McLean et al.[31] The composite ICF-AS and HFDICF have identical walls in the region between 3.5–5.2 bohr. The single-function HFD-B4 potential is no more than 3.5% from the ICF values in the range from 3.5–5.5 bohr and lies within error in the range from 5.5–6.25 bohr.

In Table V we indicate, for selected data, the predictive ability of the various argon potentials discussed in this paper. The HFD-B3 potential accurately characterizes both the microscopic and macroscopic properties which sense the well and the low and very high repulsive regions of the potential but fails to predict transport properties in the 1600–7000 K temperature range. The HFDTCS2 potential is a piece-wise potential which is formed by joining the HFD-B3 potential to the high energy beam results at its "upper range" with an exponential cubic spline. This potential predicts not only the high energy beam results of Rol, but a widely ranging set of high temperature viscosity and thermal conductivity data covering results up to 7000 K. The only data that the potential does not predict are the viscosity data of Dawe and Smith,[40] the shock-tube thermal conductivity data of Hoshino et al.[48] and Hirschberg et al.[14] It is well established that the Los Alamos viscosity data[39] are to be preferred over the Dawe-Smith data (see, for example, Aziz et al.[51]). Hirschberg[52] notes that his data in the relatively low temperature range (1550–2100 K) are 3%–4% lower than what may be deduced on the basis of kinetic theory from viscosity data in the same temperature range. He suggests that this "systematic error" may be due to boundary layers on the side walls of the shock tube. While the Hoshino et al.[48] data are consistent with the older values of Amdur and Mason,[53] they are inconsistent with the predictions of almost all empirical or model potentials. In addition, the more recent correlation of Najafi, Mason, and Kestin[42] is more consistent with the predictions of modern potentials than it is with the older data of Amdur and Mason. In other words, we can eliminate these three sets of data as valid "filters" in the assessment of potentials.

In summary, the present HFDTCS2 potential seems to overcome the dilemma of an apparent inconsistency of high energy beam with high temperature transport data. This experimental potential appears to be the best characterization of the Ar–Ar interaction for all atom–atom separations.

ACKNOWLEDGMENTS

APPENDIX: UNITED ATOM PERTURBATION THEORY RESULTS

The UAPT results were fitted[39] to the Buckingham potential form, namely,

$$V(r) = (Z_A Z_B / r)(1 + a_1 r + a_2 r^2 + a_3 r^3 + a_4 r^4 + a_5 r^5)\exp(-\alpha r), \tag{A1}$$

which is valid for $r \leqslant r_1$. The intermediate interpolation function is

$$V(r) = (Z_A Z_B / r)(1 + b_1 r + b_2 r^2 + b_3 r^3)\exp(-\beta r), \tag{A2}$$

valid for $r_1 \leqslant r \leqslant r_2$.

For argon, the parameters for Eq. (A1) are $a_1 = 9.6379$,

$a_2 = 32.7048$, $a_3 = 827.11$, $a_4 = -3310.0$,

$a_5 = 10.417$, $\alpha = 14.880$, $Z_A = Z_B = 18$.

The parameters of the interpolation function (A2) are given in Table VI.

[1] J. A. Barker, R. A. Fisher, and R. O. Watts, Mol. Phys. 21, 657 (1971).

[2] I. Amdur and J. E. Jordan, as cited in D. D. Konawolow and S. Carra, Phys. Fluids 8, 1585 (1965).

[3] I. Amdur and J. E. Jordan, Adv. Chem. Phys. X, 29(1966).

[4] P. K. Rol, as cited by R. A. Aziz in Inert Gases, edited by M. L. Klein (Springer Series in Chemical Physics, Vol. 34) (Springer, New York, 1984), Chap. 2.

[5] R. A. Aziz, Chem. Phys. Lett. 28, 47 (1974).

[6] W. L. Taylor and S. Weissman, J. Chem. Phys. 59, 1190 (1973).

[7] R. A. Aziz and H. H. Chen, J. Chem. Phys. 67, 5719 (1977).

[8] E. A. Colbourn and A. E. Douglas, J. Chem. Phys. 65, 1741 (1976).

[9] G. C. Maitland and E. B. Smith, J. Chem. Eng. Data 17, 150 (1972).

[10] K. T. Tang, J. M. Norbeck, and P. R. Certain, J. Chem. Phys. 64, 3063 (1976).

[11] A. C. Wahl and W. J. Stevens [unpublished calculations reported in part as Ref. 26 by T. L. Gilbert, O. C. Simpson, and M. A. Williamson, J. Chem. Phys. 63, 4061 (1975)]; A. C. Wahl (private communication, 1976).

[12] J. J. van den Biesen, R. M. Hermans, and C. J. N. van den Meijdenberg, Physica A115, 396 (1982).

[13] A. Cavero, K. Chung, and H. N. Powell, Proceedings of the 13th International Symposium on Shock Tubes and Waves (Niagara Falls, N. Y.), p. 297, 1981.

[14] A. Hirschberg, P. J. Vrugt, J. F. H. Willems, and M. E. H. van Dogen, Proceedings of the 13th International Symposium on Shock Tubes and Waves (Niagara Falls, N. Y.), p. 289, 1981.

[15] J. Mastovsky, CSAV Report No. Z-1026/87, Prague, Czechoslavakia 1987.

[16] H. J. M. Hanley, J. Phys. Chem. Ref. Data 2, 619 (1974).

[17] M. Ross, J. Chem. Phys. 73, 4445 (1980).

[18] M. Ross and D. A. Young, Phys. Lett. A 118, 463 (1986).

[19] A. Koide, W. J. Meath, and A. R. Allnatt, Mol. Phys. 39, 895 (1980).

[20] C. Douketis, G. Scoles, S. Marchetti, M. Zen, and A. J. Thakkar, J. Chem. Phys. 76, 3057 (1982).

[21] K. T. Tang and J. P. Toennies, J. Chem. Phys. 80, 3725 (1984).

[22] R. A. Aziz and M. J. Slaman, Mol. Phys. 58, 679 (1986).

[23] A. Kumar and W. J. Meath, Mol. Phys. 83, 3002 (1985).

[24] J. M. Standard and P. R. Certain, J. Chem. Phys. 64, 3063 (1986).

[25] E. Vogel, Ber. Bunsenges Phys. Chem. 88, 997 (1984).

[26] W. R. Wadt, J. Chem. Phys. 68, 402 (1978).

[27] R. Ahlrichs, P. Penco, and G. Scoles, Chem. Phys. 19, 119 (1977).

[28] P. J. Hay, R. T. Pack, and R. L. Martin, J. Chem. Phys. 81, 1360 (1984).

[29] R. S. Gao, L. K. Johnson, D. E. Nitz, K. A. Smith, and R. F. Stebbings, Phys. Rev. A 36, 3077 (1987).

[30] D. M. Ceperley and H. Partridge, J. Chem. Phys. 84, 820 (1986).

[31] A. D. McLean, B. Liu, and J. A. Barker, J. Chem. Phys. 89, 6339 (1988).

[32] R. A. Aziz, F. R. W. McCourt, and C. C. K. Wong, Mol. Phys. 61, 1487 (1987).

[33] R. A. Aziz, and M. J. Slaman, Mol. Phys. 57, 825 (1986).

[34] J. A. Barker, Mol. Phys. 60, 887 (1987).

[35] A. K. Dham, A. R. Allnatt, W. J. Meath, R. A. Aziz, and M. J. Slaman, Chem. Phys. (in press).

[36] R. A. Aziz and M. J. Slaman, Chem. Phys. 130, 187 (1989).

[37] A. K. Dham, A. R. Allnatt, W. J. Meath, and R. A. Aziz, Mol. Phys. 67, 1291 (1989).

[38] F. A. Guevara, B. B. McInteer, and W. E. Wageman, Phys. Fluids, 12, 2493 (1969).

[39] R. K. Pathak and A. J. Thakkar, J. Chem. Phys. 87, 2186 (1987).

[40] R. A. Dawe and E. B. Smith, J. Chem. Phys. 52, 693 (1970).

[41] H. J. M. Hanley, J. Phys. Chem. Ref. Data 2, 619 [(1974).

[42] B. Najafi, E. A. Mason, and J. Kestin, Physica 119A, 387 (1983).

[43] J. T. R. Watson, National Engineering Laboratory, East Kilbride, Glasgow, Report No. 488, 1971.

[44] S. H. P. Chen and S. C. Saxena Mol. Phys. 29, 455 (1975).

[45] N. B. Vargaftik and N. Kh. Zimina Teplofizika Vys. Temp. 2, 716 (1964).

[46] G. S. Springer and E. W. Wingeier, J. Chem. Phys. 59, 2747 (1973).

[47] D. J. Collins and W. A. Menard, J. Heat Transfer 88, 52 (1966).

[48] T. Hoshino, K. Mito, A. Nagashima, and M. Mijata, Int. J. Thermophys. 7, 647 (1986).

[49] J. Kestin, K. Knierim, E. A. Mason, B. Najafi, S. T. Ro, and M. Waldman, J. Phys. Chem. Ref. Data, 13, 229 (1984).

[50] N. B. Vargaftik, Tables on the Thermophysical Properties of Liquids and Gases, 2nd ed. (Wiley, New York, 1975).

[51] R. A. Aziz, W. J. Meath, and A. R. Allnatt, Chem. Phys. 78, 295 (1983).

[52] A. Hirschberg (private communiction, 1986).

[53] I. Amdur and E. A. Mason, Phys. Fluids 1, 370 (1958).